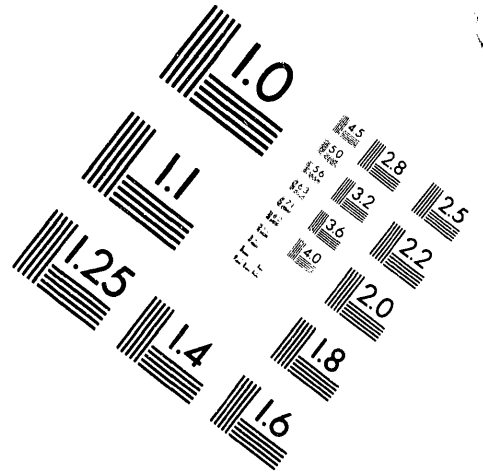
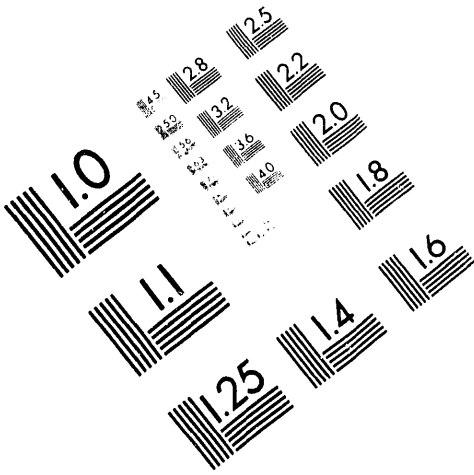




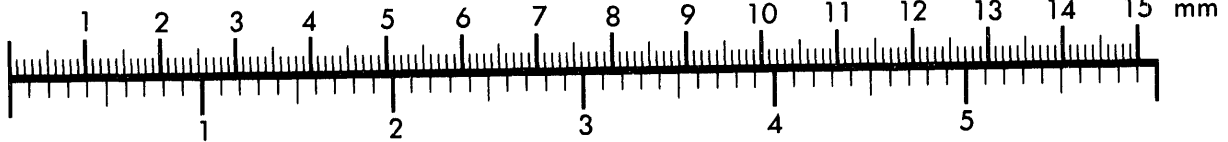
AIM

Association for Information and Image Management

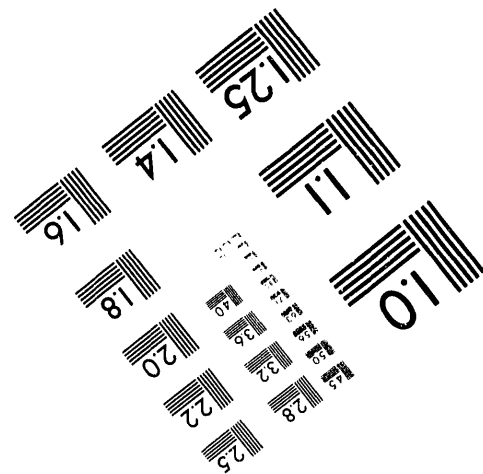
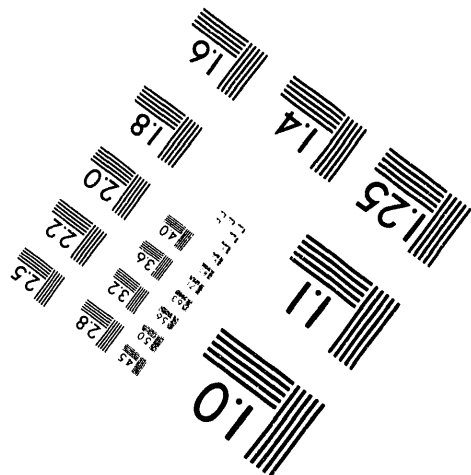
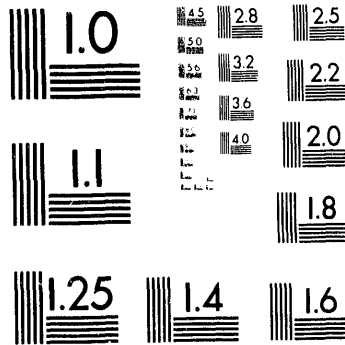
1100 Wayne Avenue, Suite 1100
Silver Spring, Maryland 20910
301/587-8202



Centimeter



Inches



MANUFACTURED TO AIM STANDARDS
BY APPLIED IMAGE, INC.

1 of 1

GA-A21167

UC-420

**LIMITS ON $m = 2, n = 1$ ERROR FIELD INDUCED
LOCKED MODE INSTABILITY IN TPX WITH
TYPICAL SOURCES OF POLOIDAL FIELD COIL
ERROR FIELD AND A PROTOTYPE CORRECTION
COIL, "C-COIL"**

by
R.J. LA HAYE

Prepared under
Contract No. DE-AC03-89ER51114
for the U.S. Department of Energy

**GENERAL ATOMICS PROJECT 3473
DATE PUBLISHED: DECEMBER 1992**

MASTER



GENERAL ATOMICS

DISTRIBUTION OF THIS DOCUMENT IS UNLIMITED ^{LB}

ABSTRACT

Irregularities in the winding or alignment of poloidal or toroidal magnetic field coils in tokamaks produce resonant low $m, n = 1$ static error fields. Otherwise stable discharges can become nonlinearly unstable, and locked modes can occur with subsequent disruption when subjected to modest $m = 2, n = 1$ external perturbations. Using both theory and the results of error field/locked mode experiments on DIII-D and other tokamaks, the critical $m = 2, n = 1$ applied error field for locked mode instability in TPX is calculated for discharges with ohmic, neutral beam, or rf heating. Ohmic discharges are predicted to be most sensitive, but even co-injected neutral beam discharges (at $\beta_N = 3$) in TPX will require keeping the relative 2, 1 error field (B_{r21}/B_T) below 2×10^{-4} . The error fields resulting from "as-built" alignment irregularities of various poloidal field coils are computed. Coils if well-designed must be positioned to within 3 mm with respect to the toroidal field to keep the total 2,1 error field within limits. Failing this, a set of prototype correction coils is analyzed for use in bringing 2,1 error field down to a tolerable level.

CONTENTS

Abstract	iii
1. Introduction	1
2. Ohmically-Heated Discharges in TPX	3
3. Neutral Beam-Heated Discharges in TPX	7
4. Radio Frequency Heated Discharges in TPX	11
5. Poloidal Field Coil Irregularity Error Fields	13
6. Prototype Correction Coils, "C-Coils"	17
7. References	19
Acknowledgment	21

LIST OF FIGURES

1. Measured critical, relative 2,1 error field versus device major radius for COMPASS-C, DIII-D, and JET with an extrapolation to ITER	5
2. Measured critical, relative 2,1 error field in DIII-D versus β for neutral beam-heated, H-mode, single-null divertor discharges	8
3. Cross section of TPX equilibrium	14
4. Helical, radial error field components from 3 mm shift of various PF coils .	16
5. Helical, radial error field spectra for C-coils CU or CL and CM with 20 kA-turns and PF coils randomly displaced by 3 mm	18

LIST OF TABLES

I. Ohmic, Deuterium Discharges, SND of $q_{95} = 3.6$ for DIII-D, DND of $q_{95} = 3.2$ for TPX	6
II. Neutral Beam-Heated, Deuterium Discharges	10
III. Predicted Parameters for TPX	13
IV. $m = 2, n = 1$ Field Error From 3 mm Horizontal Shifts	16

1. INTRODUCTION

There are now a number of experiments (Refs. 1–4) and various theoretical work (Refs. 5, 6) that are consistent on the role which resonant, low $m, n = 1$ static, magnetic error fields play on stability. An error field of the form $B_{r,mn} \cos(n\phi - m\theta)$ when applied to the plasma tends to form a static island. However, the plasma on either side of the island chain rotates due to the diamagnetic drift or to momentum injected from neutral beams or rf waves. As the plasma in the static island chain has no net flow, a torque is exerted which opposes the flowing plasma. This is balanced by viscous and inertial forces. For sufficiently small static error fields, the viscous and inertial forces dominate and inhibit the formation of a static island, *i.e.* the error field island is shrunk to a harmless size much less than expected from calculations based on a vacuum error field and a toroidally symmetric equilibrium. If the error field is increased, its torque on the flowing plasma increases, reducing the plasma slip velocity which reduces the viscous and inertial torques squeezing the static island. At a critical condition, the error field torque is sufficient to stop flow around the resonant surface and penetration and reconnection occur. This is a locked mode, *i.e.* the plasma response to the static error field changes state from the rotating plasma squeezing the vacuum island into a negligible size (Refs. 5, 6) to the locked plasma amplifying the vacuum island by a large factor (Refs. 5–8). Disruptions usually follow locked modes when the edge safety factor is less than $q = 4$. For reliable, steady-state discharges without disruptions, locked modes must be avoided; this is done by keeping static error fields, particularly the $m = 2, n = 1$ component, well below the critical level.

In Section 2, the theory and experiments for low density, ohmic locked modes are presented and extrapolated to TPX. In Section 3, the critical error field in TPX for high beta, neutral beam-heated discharges is calculated. In Section 4, high beta, rf-heated discharges are considered. In Section 5, the Fourier spectra for typical poloidal field coil irregularities are given with a total 2,1 field error criterion on coil alignment. In Section 6, a prototype correction coil, “C-coil” is analyzed.

2. OHMICALLY-HEATED DISCHARGES IN TPX

The nonlinear tearing theory of the interaction of static resonant magnetic perturbations with the rotating plasma has been examined by Fitzpatrick and Hender. A critical radial, helical error field evaluated at minor radius $r = a$ relative to toroidal field B_T is predicted for $m = 2, n = 1$ (Ref. 5).

$$\frac{B_{r\ 21}}{B_T} \Big|_a \approx 4.2 g^2 \left[\left(\frac{r_s}{R_0} \right)^{1/3} \left(\frac{-\Delta'_0 r_s}{S} \right)^{1/3} \right] \times (f \tau_H)^{4/3} \quad , \quad (1)$$

where g^2 is a weak function of viscosity of order one; r_s is the resonant surface minor radius for $q = 2$; $-\Delta'_0 r_s$ and S are the dimensionless tearing parameter and shear at r_s ; f is the natural unperturbed toroidal rotation frequency at $q = 2$; and $\tau_H = R_0 (\mu_0 \bar{n} m_i)^{1/2} / B_T$ is the Alfvén time. Equation (1) predicts that slower rotating plasmas (lower f) are more easily locked. The term $(f \tau_H)^{4/3}$ scales as $(f R / B_T)^{4/3} \bar{n}^{2/3}$, thus lower density plasmas are easier to lock because of weaker inertial forces; the g^2 factor increases as viscous forces become more important. The theory is successful in explaining ohmic experimental results that:

1. Critical $B_{r\ 21} / B_T \sim \bar{n}^{2/3}$ in ohmic discharges.
2. That lower q discharges with more unstable tearing profiles have lower critical $B_{r\ 21} / B_T$.
3. That larger devices with slower rotation have lower critical $B_{r\ 21} / B_T \sim f^{4/3}$.

For ohmic plasmas, f is about the electron diamagnetic drift frequency (Ref. 4)

$$f \approx \kappa_B T_{e0} / e B_T a^2 \quad , \quad (2)$$

with the central electron temperature for parabolic squared profile with elongation κ

$$T_{eo} \text{ (eV)} \approx 4.2 \times 10^6 \left(\frac{\tau_{Ee}}{\bar{n}} \right)^{2/5} \left(\frac{I_p}{\kappa \pi a^2} \right)^{4/5} Z_{\text{eff}}^{2/5}, \quad (3)$$

and electron energy confinement time that of Pfeiffer-Waltz (Ref. 9)

$$\tau_{Ee} = 9.5 \times 10^{-20} \bar{n}^{0.90} a^{0.90} R_0^{1.63} Z_{\text{eff}}^{0.23}, \quad (4)$$

where all quantities are MKS unless otherwise noted.

Using Eqs. (2) through (4), the predicted frequency $f \sim R_0^{-9/5} B_T^{-1/5}$ and is a strongly decreasing function of device size (Ref. 4). Thus by Eq. (1), the critical error field decreases rapidly with increasing device major radius. This is confirmed experimentally in a matched set of critical 2,1 error field experiments in COMPASS-C, DIII-D and JET with $R_0 = 0.56$ m, 1.67 m, and 3.0 m respectively (Refs. 4, 10). Keeping the edge safety factor $q \approx 3.5$, with deuterium ohmic discharges and similar normalized low density of $\bar{n} \pi a^2 / I \approx 0.2 \times 10^{20} \text{ m}^{-3} \times \text{m}^2 / \text{MA}$ [0.2 of Greenwald limit (Ref. 11)], the critical $B_{r,21}/B_T$ measured decreased rapidly with increasing device major radius as shown in Fig. 1. The extrapolation to a $R_0 = 6$ m ITER is also plotted.

For detailed comparison of the model to the high-current double-null design-basis of TPX, we scale DIII-D at $R_0 = 1.67$ m and $B_T = 1.3$ T to TPX at $R_0 = 2.25$ m and $B_T = 4.0$ T (Ref. 12). The model predictions for DIII-D and TPX for ohmic discharges are shown in Table I. The model based on Eqs. (1) to (4) is in good agreement with DIII-D measurements. One assumes that for similar edge safety factor, current profiles will be similar so that r_s/R_0 , $-\Delta'_0 r_s$ and S will be the same. Taking $r_s/R_0 = 0.29$, $-\Delta'_0 r_s = 0.5$ and $S = 1$, the theory of Eq. (1) predicts for DIII-D that $B_{r,21}/B_T|_{\text{crit}} = 3.2 \times 10^{-4}$ compared to 1.7×10^{-4} measured. As the current profile parameters of the elongated DIII-D single-nulled divertor are only approximately known and the theory is for a straight, cylindrical plasma, the theory is quite successful in predicting absolute values of critical error field.

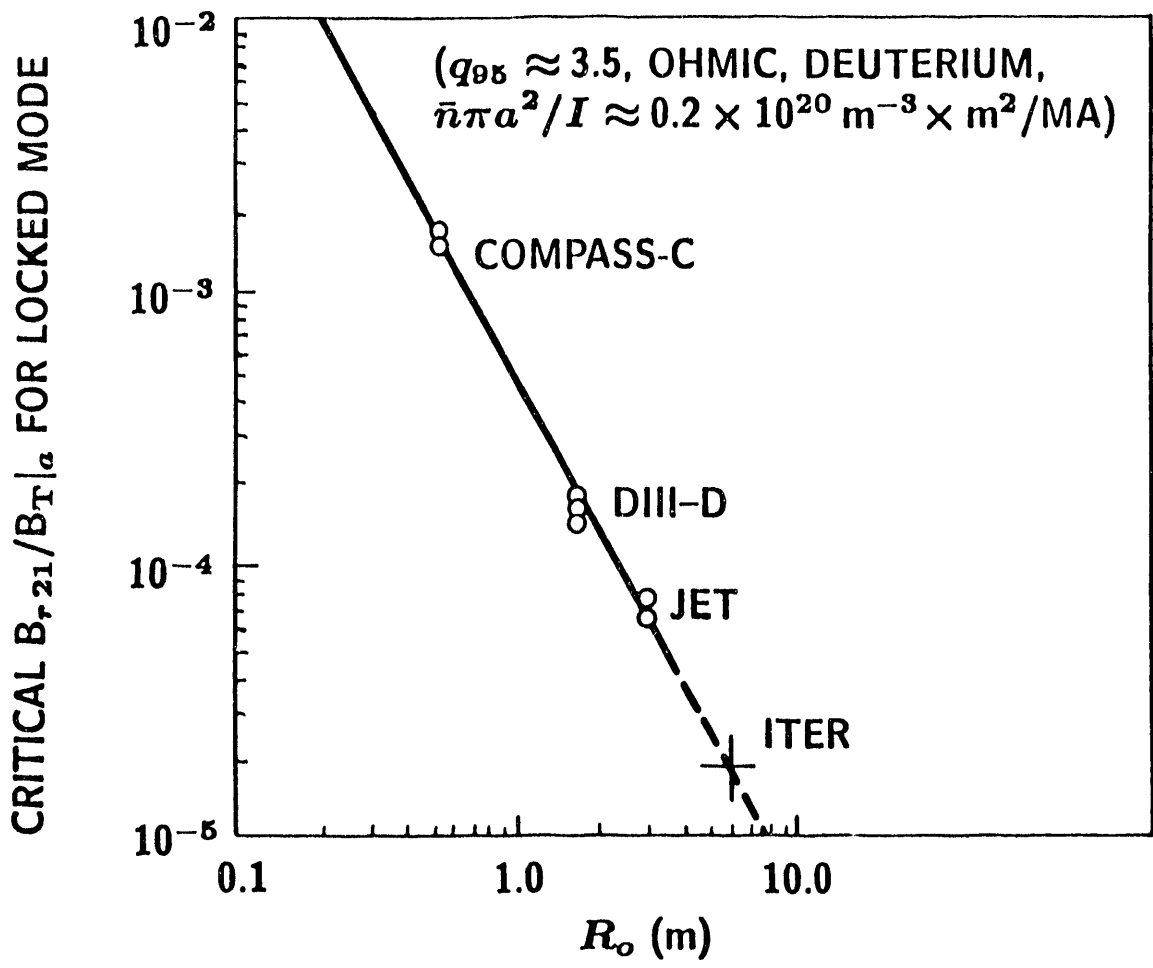


Fig. 1. Measured critical, relative 2,1 error field versus device major radius for COMPASS-C, DIII-D, and JET with an extrapolation to ITER. All experiments keep edge safety factor $q \approx 3.5$, normalized density $\bar{n} \pi a^2 / I \approx 0.2 \times 10^{20} \text{ m}^{-3} \times \text{m}^2 / \text{MA}$ and are done in ohmic, deuterium discharges.

TABLE I
OHMIC, DEUTERIUM DISCHARGES, SND OF $q_{95} = 3.6$ FOR DIII-D,
DND OF $q_{95} = 3.2$ FOR TPX, $Z_{\text{eff}} = 2$, $\bar{n} \pi a^2 / I_p = 0.24$ ($10^{20} \text{ m}^{-3} \times \text{m}^2 / \text{MA}$)

	DIII-D	TPX
R_0 (m)	1.67	2.25
a (m)	0.64	0.50
κ	1.6	2.0
B_T (T)	1.3	4.0
I_p (MA)	0.95	2.0
\bar{n} (10^{20} m^{-3})	0.18	0.51
τ_{Ee} (s) (Pfeiffer-Waltz)	0.037	0.12
T_{eo} (keV)	0.98	2.4
f_s (kHz)	1.8	2.4
g^2	3.1	1.7
$\left. \frac{B_{r21}}{B_T} \right _a$ crit	1.7×10^{-4} (measured)	0.9×10^{-4} (predicted)

To keep the ohmic target plasmas in TPX from having locked modes and disruption before the supplementary heating phase, the 2,1 relative error fields must be kept at or below 0.9×10^{-4} for $\bar{n} \pi a^2 / I_p \approx 0.2$. As $B_{r21} / B_T \sim \bar{n}^{2/3}$, operating at $\bar{n} \pi a^2 / I_p \approx 0.6$ increases the allowable error field by a factor of $3^{2/3} \approx 2$ but may obviate the use of desirable low density, ohmic target plasmas.

3. NEUTRAL BEAM-HEATED DISCHARGES IN TPX

For discharges with co-injected neutral beams, the rotation depends on the beam angle, power and voltage. Critical 2,1 error fields were experimentally determined in single-null divertor (SND), ELMing H-mode discharges in DIII-D (Ref. 13). The basic parameters were similar to those of Table I except that frequency and density were weak functions of beam power. The density was medium-high at $\bar{n} \pi a^2 / I_p \simeq 0.6$. The critical relative error field was found to drop sharply with increasing power and beta as shown in Fig. 2. This was interpreted as due to the 2,1 tearing stability parameter approaching zero as β went to $\beta_{\max} \simeq 3.5 I \text{ (MA)} / a B_T$, *i.e.* as β went up, $-\Delta'_0 \tau_s$ went down to zero from positive stable value. As a result, near the beta limit the critical 2,1 error field dropped to below the ohmic value despite the much faster rotation.

The DIII-D results with 75 keV beams are scaled to TPX at $R_0 = 2.25$ m, $B_T = 4.0$ T with 100 keV beams. For H-mode discharges the natural 2, 1 toroidal frequency f is determined by the beam momentum input and the viscous losses (Ref. 13).

$$f \approx \frac{1}{2\pi R_0} \left(\frac{v_B P_B \cos \psi_B}{eV_B} \right) \frac{\tau_M}{2\pi R_0 \kappa \pi a^2 \bar{n}} \quad , \quad (5)$$

where v_B is the beam neutral particle speed, V_B is the beam voltage, P_B is the beam power, ψ_B is the beam angle and τ_M is the momentum confinement time taken as equal to the JET/DIII-D H-mode total energy confinement time (Ref. 14).

$$\tau_M \equiv \tau_E = 4.03 \times 10^{-5} P_B^{-0.46} I_P^{1.03} R_0^{1.48} \quad , \quad (6)$$

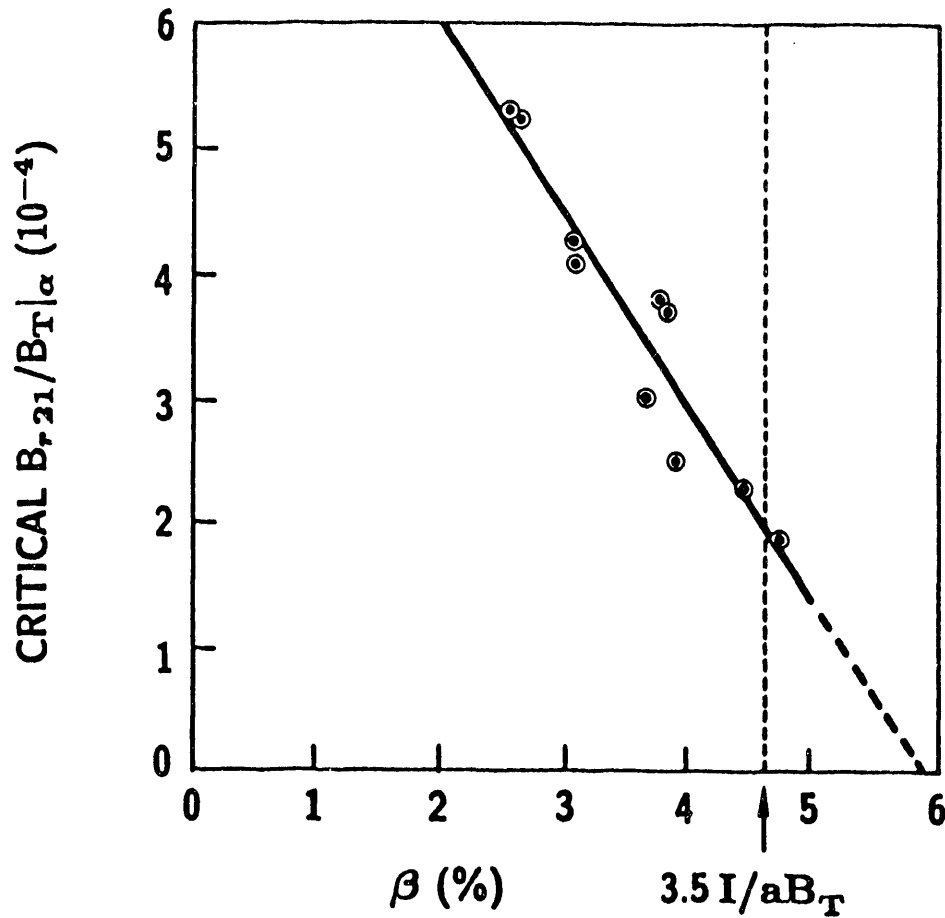


Fig. 2. Measured critical, relative 2,1 error field in DIII-D versus β for neutral beam-heated, H-mode, single-null divertor discharges with $q_{95} = 3.5$ and $\bar{n} \pi a^2 / I \approx 0.6 \times 10^{20} \text{ m}^{-3} \times \text{m}^2 / \text{MA}$.

with all parameters in MKS units. For flat density profile, parabolic temperature profile and $T_e = T_i$,

$$T_{e0} \text{ (eV)} = \beta B_T^2 / 3 \bar{n} \kappa_B \mu_0 \quad . \quad (7)$$

The predicted theoretical, critical, relative 2,1 error field for large, beam driven tokamaks where viscous drag dominates is (Ref. 5)

$$\left. \frac{B_{r21}}{B_T} \right|_a = 1.1 \left[\left(\frac{r_s}{R_0} \right)^{1/5} (-\Delta'_0 r_s)^{3/5} S^{1/5} \right] \left(\frac{f \tau_H^2}{\tau_M} \right)^{2/5}, \quad (8)$$

which scales as $(f R^2 / B_T^2 \tau_M)^{2/5} \bar{n}^{2/5}$. Again, more slowly rotating, lower density discharges are predicted to be more sensitive to error field induced locked modes. Note that for NB discharges, if $f \sim \bar{n}^{-1}$, B_{r21}/B_T has no explicit dependence on density.

The model predictions for neutral beam-heated, deuterium, ELMing, H-mode, SND discharges for DIII-D and DND discharges for TPX are shown in Table II. The calculations take $\bar{n} \pi a^2 / I_p = 0.6$ ($10^{20} \text{ m}^{-3} \times \text{m}^2 / \text{MA}$) $\beta_N \equiv 3$ [$\beta_N = 3 I_p$ (MA) / $a B_T$ with $\beta = 2 \mu_0 (P_B \tau_E) / B_T^2 V$ and $V = 2 \pi R_0 \kappa \pi a^2$] and $T_e = T_i$ with $V_B = 75$ keV for DIII-D, 100 keV for TPX, and $\psi_B = 47^\circ$. The model predictions shown for τ_E , T_{eo} and f for DIII-D are in good agreement with measurements. The measured critical $B_{r21}/B_T \Big|_a$ of 3.0×10^{-4} is in agreement with theory of Eq. (8) for $r_s/R_0 = 0.26$, $-\Delta'_0 r_s \Big|_a = 0.22$ and $S = 1$. Scaling to TPX, one predicts critical $B_{r21}/B_T \Big|_a = 2.2 \times 10^{-4}$, somewhat lower than measured in DIII-D for $\beta_N = 3$ and the same current profile. The rotation frequency f is higher and the Alfvén time is lower. As usually noted both experimentally and theoretically, major radius scaling dominates in determining the critical 2,1 error field. Thus TPX will not be too different than DIII-D.

TABLE II
 NEUTRAL BEAM-HEATED, DEUTERIUM DISCHARGES,
 H-mode, $\bar{n} \pi a^2 / I_p = 0.60$ ($10^{20} \text{ m}^{-3} \times \text{m}^2 / \text{MA}$), $\beta_N = 3$, $T_e \equiv T_i$

	DIII-D	TPX
R_0 (m)	1.67	2.25
a (m)	0.60	0.50
κ	1.8	2.0
B_T (T)	1.2	4.0
I_p (MA)	0.95	2.0
\bar{n} (10^{14} m^{-3})	0.50	1.5
P_B (MW)	5.9 (75 kV)	27 (100 keV)
τ_E (s)	0.095	0.16
(JET/DIII-D, H)		
T_{eo} (keV)	1.9	5.3
f_s (kHz)	5.7	9.1
$\frac{B_{r21}}{B_T} \Big _{a_{crit}}$	3.0×10^{-4} (measured)	2.2×10^{-4} (predicted)

4. RADIO FREQUENCY HEATED DISCHARGES IN TPX

For rf-heated discharges, one assumes: (1) equal confinement and profiles as for neutral beams, (2) no net momentum input and (3) that the 2,1 natural toroidal rotation frequency f is that of the electron diamagnetic drift but with parabolic T_e profile,

$$f \approx 2 \kappa_B T_{eo} / 3 e B_T a^2 \quad , \quad (9)$$

For the parameters of Table II, $f = 3.5$ kHz is predicted for rf discharges and scaling from DIII-D to TPX, $B_{r21}/B_T \sim (f R^2 / B_T^2 \tau_M)^{2/5} \bar{n}^{2/5}$ one predicts critical $B_{r21}/B_T \approx 1.5 \times 10^{-4}$ for rf TPX discharges, lower than for the 100 keV neutral beam discharges injected at 47° . The slower rotation is the cause of the predicted greater sensitivity as everything else is assumed equal.

5. POLOIDAL FIELD COIL IRREGULARITY ERROR FIELDS

The normalized density, predicted 2,1 natural toroidal rotation frequency, Alfvén time, momentum confinement time and critical relative error field are given for TPX in Table III. The ohmic error field presents the biggest potential problem but reliable, steady-state operation of TPX without error field-induced locked modes and disruptions requires staying well below critical values for beams. The estimated, critical 2,1 error field is evaluated on a circular torus. To account for toroidal and elongation effects on real, non-circular flux surfaces, one must also limit $n = 1, m = 1, 3,$ and 4 error fields to at or below the 2,1 limit. Careful coil design and alignment as well as error field correcting coils will be necessary to avoid error field-induced locked modes and disruption on TPX.

TABLE III
PREDICTED PARAMETERS FOR TPX

	Ohmic	RF	Neutral Beam
$\bar{n} \pi a^2 / I_p$ ($10^{20} \text{ m}^{-3} \times \text{m}^2 / \text{MA}$)	0.2	0.6	0.6
f (kHz)*	-2.4	-3.5	9.1
τ_H (μs)	0.26	0.45	0.45
τ_M (s)	0.12	0.16	0.16
$B_{r21} / B_T _a$ (10^{-4})	0.9	1.5	2.2

*Negative frequency is electron diamagnetic drift direction.

The cross section of a TPX high current double-null divertor (DND) equilibrium and PF coil set at the start of plasma current flattop is shown in Fig. 3 (Ref. 12). To

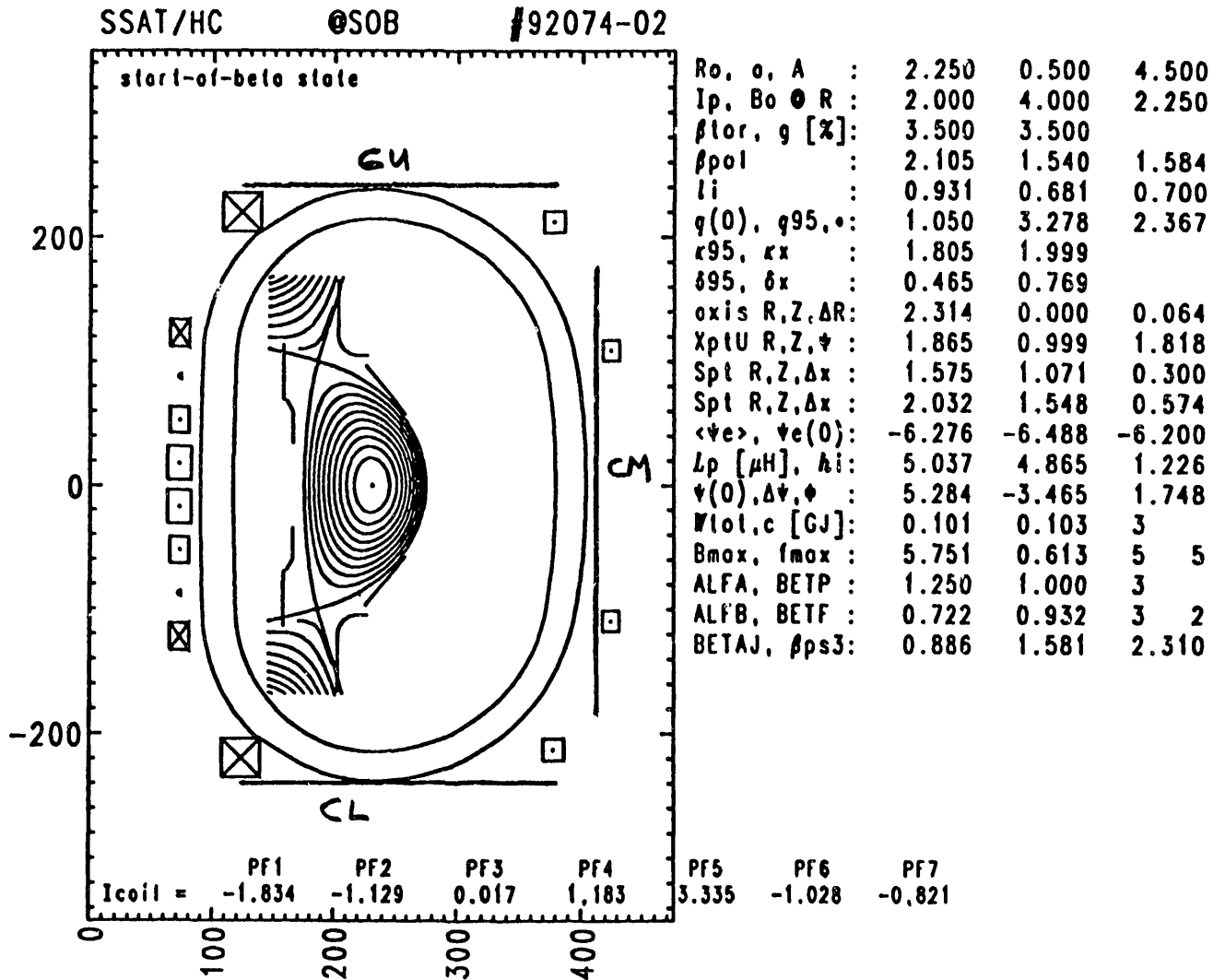


Fig. 3. Cross section of TPX equilibrium. Also shown are prototype "window-pane" correction coils, CU, CM, and CL.

study field errors, coils PF1U, PF5U, and PF6U are individually shifted by $\Delta R = 3$ mm each, *i.e.* horizontally with respect to the toroidal field as likely alignment errors in assembly. Previous work on DIII-D etc. indicates that $\Delta Z = 3$ mm tilts will produce similar $n = 1$ error fields. The $n = 1, m$ spectrum of each “as-built” irregularity is Fourier analyzed on a circular torus of major radius $R_0 = 2.25$ m and minor radius $\sqrt{2}a = 0.71$ m to allow for the $\kappa = 2$ elongation. Table IV lists coil positions R_c, Z_c , current I_c and $m = 2, n = 1$ helical radial field error $B_{r,21}$. The $n = 1, m$ spectra of $B_{r,mn}$ are shown in Fig. 4. The inner PF coils produce the largest $B_{r,21}$ for a given misposition from the ideal location.

Ignoring any toroidal field coil errors, PF coils other than 1,5 and 6 U and L, and any winding irregularities such as from feeds, turn-to-turn transitions etc., one can now set a limit on alignment error taking total $B_{r,21}/B_T \leq 9.9 \times 10^{-4}$ or $B_{r,21} \leq 3.6$ G. Assuming random shifts and tilts of each of the six studied coils (PF1U, PF1L, PF5U, PF5L, PF6U, and PF6L) the allowable alignment error by the method of the square root of the sum of the squares total is $\Delta S \equiv [(\Delta R)^2 + (\Delta Z)^2]^{1/2} \leq 3$ mm. Of course, the DIII-D experience is that errors are not random as an assembly misalignment in one coil can propagate to misalign the next coil placed in position (Ref. 15). Allowing for inevitable “as-designed” winding irregularities will make the tolerable ΔS for alignment even lower.

TABLE IV
 $m = 2, n = 1$ FIELD ERROR FROM 3 mm HORIZONTAL SHIFTS

Coil	R_c (m)	Z_c (m)	I_c (MA)	B_{r21} (G)
PF1U	0.72	0.18	-2.42	1.63
PF5U	1.23	2.20	3.40	0.71
PF6U	3.78	2.13	-1.60	0.39

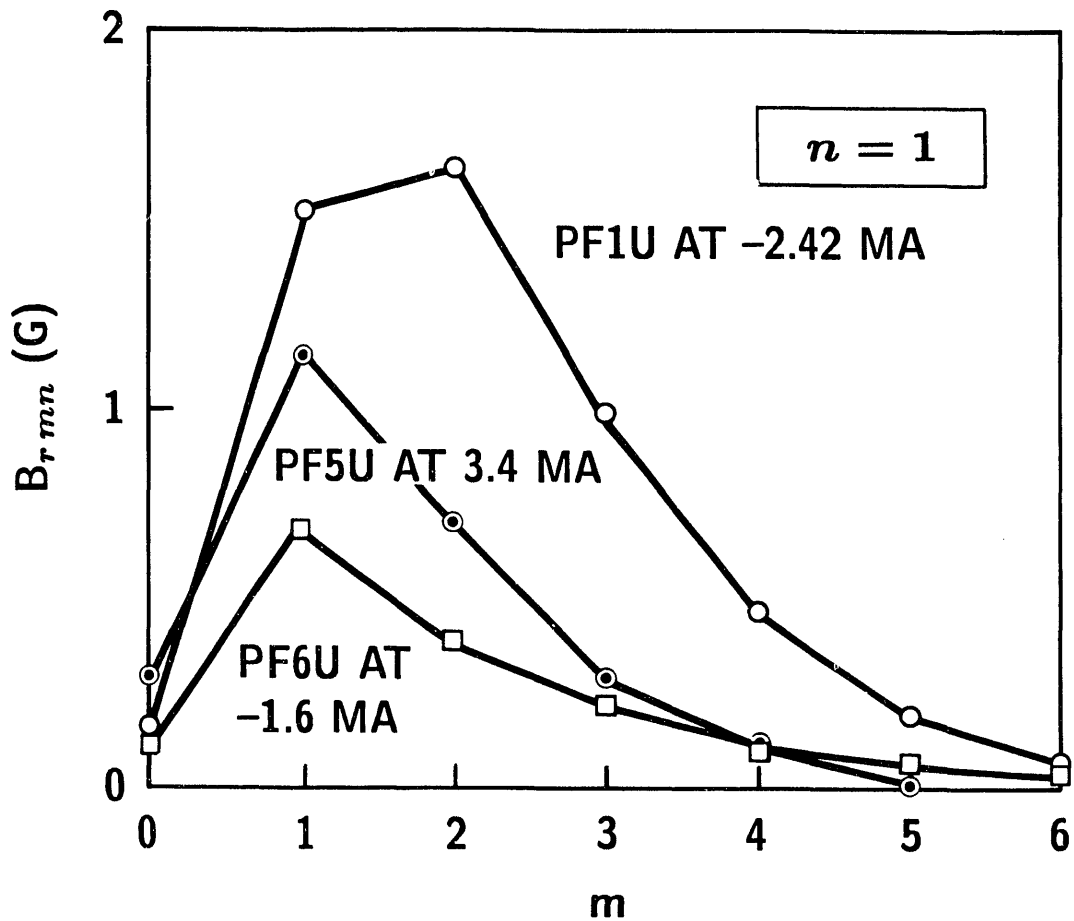


Fig. 4. Helical, radial error field components from 3 mm shift of various PF coils.

6. PROTOTYPE CORRECTION COILS, "C-COILS"

To reduce error fields a simple correction coil, the " $n = 1$ coil" has been useful on DIII-D and a more effective coil is planned (Refs. 1, 16). Prototype "window-pane" coils such as planned for DIII-D and contemplated for BPX may be needed for TPX. The conceptual set of "C-coils" places four windowpanes on top, four on the bottom, and four on the outside of TPX. See Fig. 3. Each windowpane C-coil segment is 80° in toroidal extent and with opposite pair in opposition an $n = 1$ correcting field is produced with some $n = 3$ sideband. The Fourier analyses of one of each pair of each type is shown in Fig. 5 for 20 kA-turns along with the error field spectrum for random 3 mm displacements of the PF-coils. The proposed C-coils have similar $n = 1, m$ spectra as typical PF coil alignment errors and can thus be appropriately driven so as to reduce or null the $n = 1, m = 1, 2,$ and 3 error field components. The 20 kA-turns current limit for the C-coil is very modest compared to the PF coil currents.

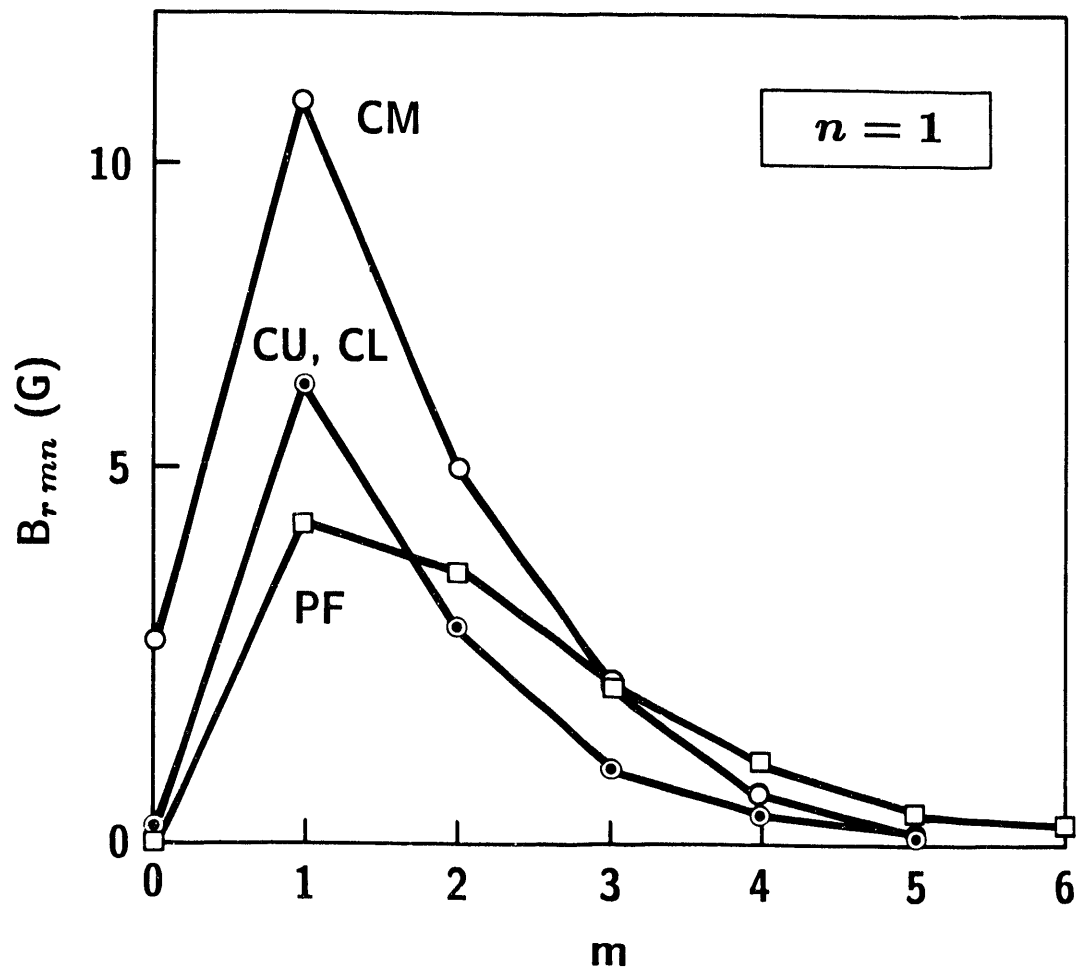


Fig. 5. Helical, radial error field spectra for C-coils CU or CL and CM with 20 kA-turns and for PF coils randomly displaced by 3 mm.

7. REFERENCES

1. Scoville, J.T., La Haye, R.J., Kellman, A.G., Osborne, T.H., Stambaugh, R.D., Strait, E.J., and Taylor, T.S., Nucl. Fusion **31**, 875 (1991).
2. Morris, A.W., Carolan, P.G., Hender, T.C., and Todd, T.N., Phys. Fluids B **4**, 413 (1992).
3. Fishpool, G.M., Campbell, D.J., Fitzpatrick, R., and Haynes, P.S., "A Locked Mode Associated With Low Density in JET," Proceedings of IAEA Technical Committee Meeting on Avoidance and Control of Tokamak Disruptions, September 10–12, 1991, (IAEA, Vienna, 1992), p. 84.
4. La Haye, R.J., Fitzpatrick, R., Hender, T.C., Morris, A.W., Scoville, J.T., and Todd, T.N., Phys. Fluids B **4**, 2098 (1992).
5. Fitzpatrick, R., and Hender, T.C., Phys. Fluids B **3**, 644 (1991).
6. Jensen, T.H., Leonard, A.W., and Hyatt, A.W., "A Simple Model for Driven Islands in Tokamaks," General Atomics Report GA-A20980, August 1992, submitted to Phys. Fluids B.
7. Lee, J.K., Ikezi, H., McClain, F.W., and Ohya, N., Nucl. Fusion **23**, 63 (1983).
8. Reiman, A., and Monticello, D., Phys. Fluids B **3**, 2230 (1991).
9. Pfeiffer, W.W., and Waltz, R.E., Nucl. Fusion **19**, 51 (1979).
10. Todd, T.N., *et al.*, Tuda, T., *et al.*, and La Haye, R.J., *et al.*, "The Study and Control of Error-Field Induced Locked Modes in Tokamaks," Proceedings of the Fourteenth International Conference on Plasma Physics and Controlled Nuclear Fusion Research, (IAEA, Würzburg, Germany, 1992) to be published.

11. Greenwald, M., Terry, J.L., Wolfe, S.M., Ejima, S., Bell, M.G., Kaye, S.M., and Neilson, G.H., Nucl. Fusion **28**, 2199 (1988).
12. Bulmer, R., and Pearlstein, N., Memo of November 9, 1992, "TPX/SSAT Design Basis Equilibria."
13. La Haye, R.J., Hyatt, A.W., and Scoville, J.T., "Non-Linear Instability to Low m , $n = 1$ Error Fields in DIII-D as a Function of Plasma Fluid Rotation and Beta," General Atomics Report GA-A20824, May 1992, to be published in Nucl. Fusion.
14. Ryter, F., Schissel, D.P., Gruber, O., Kardaun, O.J.W.F., Menzler, H.P., *et al.*, "Expression for the Thermal H-Mode Energy Confinement Time Under ELM-Free Conditions," General Atomics Report GA-A20707, September 1992, submitted to Nucl. Fusion.
15. La Haye, R.J., and Scoville, J.T., Rev. Sci. Instrum. **62**, 2146 (1991).
16. Scoville, J.T., and La Haye, R.J., "Design of a Coil to Correct Magnetic Field Errors on the DIII-D Tokamak," General Atomics Report GA-A20577, 1991, and published in Proc. 14th IEEE/NPSS Symposium on Fusion Engineering, San Diego, California, 1991, Vol. 2, p. 1144.

ACKNOWLEDGMENT

This work was supported by the U.S. Department of Energy under Contract No. DE-AC03-89ER51114.

**DATE
FILMED**

8 / 23 / 93

END

